

Influence of 3D Printed Elastic Structures on the Pressure Pulsations in the Reciprocating Compressor Manifold



Damian Brewczyński , Kamil Chmielarczyk, Jarosław Błądek, and Przemysław Młynarczyk

Abstract In recent years, there has been several research describing the influence of elastic elements, such as springs or flexible polymers, on the damping of pressure pulsations. As pressure pulsations are one of the most inconvenient phenomena occurring in positive displacement compressor installations, experimental studies of various elastic elements produced with 3D printing techniques were carried out. The research focusses on the description of the relationship between the geometrical parameters of the printed springs and their impact on the pressure pulsations in the installation. The presented studies are basically preliminary studies that allow to estimate the possible direction of further development of such methods in the field of pressure pulsation damping.

Keywords 3D printing · Springs · Pressure pulsations · Damping

1 Introduction

With the increasing use of variable capacity compressors operating in continuous operation, a new challenge has arisen in damping pulsations, which in this situation have different frequencies. One of the proposed methods is the installation of nozzles produced with 3D printing techniques in the compressor discharge manifold [1]. Another interesting solution, described in scientific studies, is the possible effective suppression of peak-to-peak value of the compressed gas pulsation by a flexible element in the form of a spring [2]. The authors of this paper concludes that the overall reduction of the pressure pulsation can be obtained in this way. In particular, it was highlighted that the highest damping is obtained when the pulsation frequency corresponds to the longitudinal natural frequency of the spring. Therefore, it should be possible to design such a flexible shape that will have a simultaneous

D. Brewczyński · K. Chmielarczyk · J. Błądek · P. Młynarczyk (✉)
Faculty of Mechanical Engineering, Cracow University of Technology, Cracow, Poland
e-mail: pmlynarczyk@pk.edu.pl

effect on the damping of pressure pulsations through geometrical interaction with the flowing medium and through characteristics related to the natural longitudinal frequency. Testing whether printed springs can act in this way is the first step towards the development of a new technology. 3D printing allows to make any shape, and therefore also springs with appropriate parameters. There are studies in the literature on determining the elastic properties of prints. One solution is to create monolithic mechanisms having elastic backlash-free rotating pairs (joints). Such mechanisms can be immediately equipped with flat springs [3]. 3D printed components also make it possible to optimise damping elements. It is possible to increase the damping coefficient of a printed element by almost 80% relative to a solid element of the same mass. This is possible, among other things, by using a shape based on the geometry of the bonding of carbon atoms in graphene and the use of a negative Gaussian curve shape [4]. Making deformable components using 3D printing methods allows the design of structures in which the directions and degree of possible deformation can be precisely controlled. It is possible to create a component that, for example, only deforms linearly in the vertical direction and allows bending in only one plane [5]. As 3D printing technology allows for the creation of geometries that are impossible with other manufacturing techniques, the authors [6] succeeded in designing and manufacturing components with a negative Poisson's ratio. Very interesting is work [7], where by using several different materials when printing a single object, it is possible to control the behaviour of the component, the degree of deformation and damping. In this way, origami-inspired structures were designed and manufactured, the properties of which can be precisely designed by appropriately arranging rigid and elastic fragments in a single part.

Using additive manufacturing techniques (3D printing), you can completely print the spring element together with the fastening elements as one object. As for the modulus of elasticity and the damping coefficient, they depend on the selected 3D printing technology, the type of selected material, the designed geometry, the part's filling density and the type and procedure of finishing the printed element. The two most popular printing techniques today are FDM/FFF and SLA. To obtain the expected print properties, many different parameters can be manipulated during the 3D printing process. In the FDM/FFF technology, we can manipulate parameters such as the type of material, printing temperature, degree of print cooling (adhesion between layers), the number of solid coatings, layer height as well as the percentage and geometry of filling. The parameters of the material itself are provided by the manufacturer, while taking into account that in the FDM/FFF technology the material is thermally treated during printing, it is reasonable to conduct material tests after printing with the set parameters.

In the SLA technology, which uses photopolymers for printing, in addition to the type of material, we can modify the properties of the print by changing the intensity of UV light exposure during finishing processing. This technology is much more accurate than FDM. Unfortunately, it is also associated with a much more difficult process of print preparation and finishing.

On the other hand, is characterized by the lowest cost among 3D printing technologies and, with small objects, the shortest time from idea to physical object. This

is due to the fact that after printing the element usually does not require additional processing. The limitation is the low accuracy of model mapping and the highly anisotropic structure of the printed parts. Objects printed in this technology have a much lower strength in the Z-direction between the layers, thus SLA technology is more appropriate for spring printing. However, for SLA printed springs, it is definitely more difficult to determine the natural frequency, compared to steel springs, because the material parameters are strongly dependent on the method of processing the printouts. In this paper, the authors present the results of research aimed at assessing the possibility of damping a specific harmonic frequency of pressure pulsation that occurs in the installation using printed springs with different characteristics.

2 3D Printed Elastic Structures

For compressor installation, 6 models were designed and made in the SLA 3D printing technology.

Each of the models had the same mounting rings made in one print together with a part of the spring that matched the internal diameter in the installation. In order to allow free movement of the spring section, each model has a 1 mm gap between the inside of the pipe in the system and the spring section of the damper.

The shape and size of the helical/spiral sketch were the only variables between the models. Three basic shapes were selected, which are shown in Fig. 1. Circle, rectangle with side proportions 2:1 and ellipse with diameter proportions 2:1.

The pitch of the helix/spiral in all models was the same and equal to 20 mm. The spring section had a length of 135 mm. At its ends, fastening rings, each 5 mm high, were designed, as shown in Fig. 2.

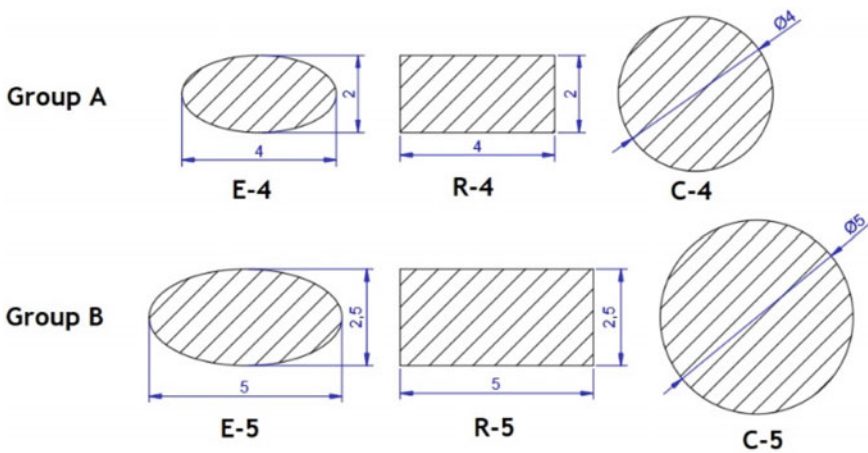


Fig. 1 Sketches of helical/spiral cross-sections

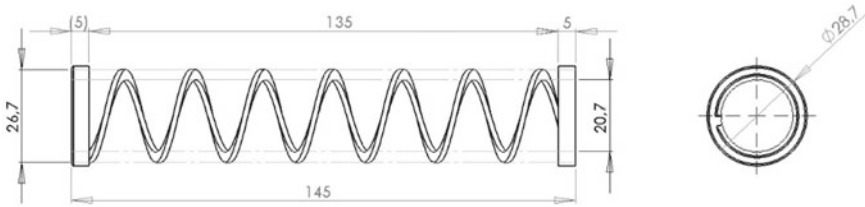


Fig. 2 An element from group “A” with a rectangular sketch sweep along the helix

The springs were designed in 2 groups. Group “A” had 4 mm sketch dimension along X-axis swept along helix/spiral. Group “B” had 5 mm sketch dimension along X-axis swept along helix/spiral. The groups were created in such a way that in a given group the percentage of covering the clearance in the installation was the same. In group “A” it was 33.9%, in group “B” it was 47.3%.

2.1 3D Printing Process Details

Parts designed in SolidWorks were imported into the PreForm programme. Printing an element such as a spring requires many support points in the SLA printing technology (Fig. 3). The supports had to be designed to hold the part rigidly during printing. The correct placement of the support structures was crucial for proper printing. If the support structures were too weak or in the wrong places, the printed element would undergo undesirable deformation already at the printing stage. If there were too many support structures or in the wrong places, they could be impossible to remove during final processing. A relatively large amount of time was devoted to the support design stage to ensure a successful print on the first attempt.

The elements were printed on a Formlabs Form 3 printer from Standard Gray photopolymer. The layer height has been set to 0.05 mm for high accuracy. With the given dimensions of the part and the layer height of 0.05 mm, printing one element took about 13 h.

In SLA technology, the part after printing is not yet suitable for use. After the printed part from the platform, the part should be cleaned of uncured resin. The resin is toxic and can cause chemical irritation; therefore, it is necessary to use protective measures and a separate washing station. The parts were washed from the uncured resin in a circulating and ultrasonic washer containing 99% pure isopropyl alcohol. The parts are then dried at room temperature overnight. Only after this process can the part be safely taken in hand.

The next step is the mechanical removal of the support structures. This process uses cutters, scalpels and precision grinders, the process of removing structures is shown in Fig. 4.

The last stage is curing the outer surface of the part with UV lamps. The photopolymerization process using UV light is an exothermic process. The high temperature

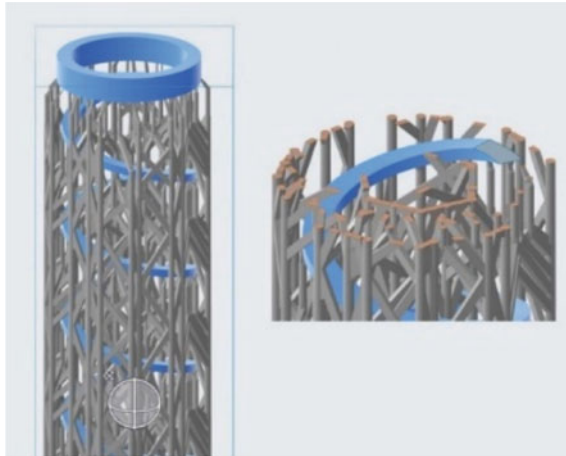


Fig. 3 Visualization from PreForm program. The blue color represents the printed element, the gray color represents the support structures

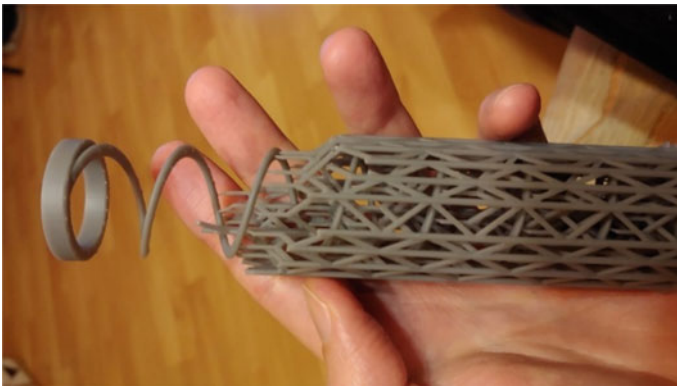


Fig. 4 An element during the removal of support structures

generated during this process could distort the processed parts, therefore the process was carried out using a specially designed form to prevent deformation (Fig. 5). The printed element fixed in the specially designed form was cured with UV light in water to allow heat dissipation.

2.2 *Determination of the Spring Stiffness Coefficient*

For the part prepared in this way, the stiffness coefficient was tested and then mounted in the measuring installation to carry out tests allowing for estimation of the influence



Fig. 5 Elements, after removal of support structures, fixed in forms and prepared for curing with UV light

of the printed spring on pressure pulsation. The stand for measuring the stiffness coefficient is shown in Fig. 6.

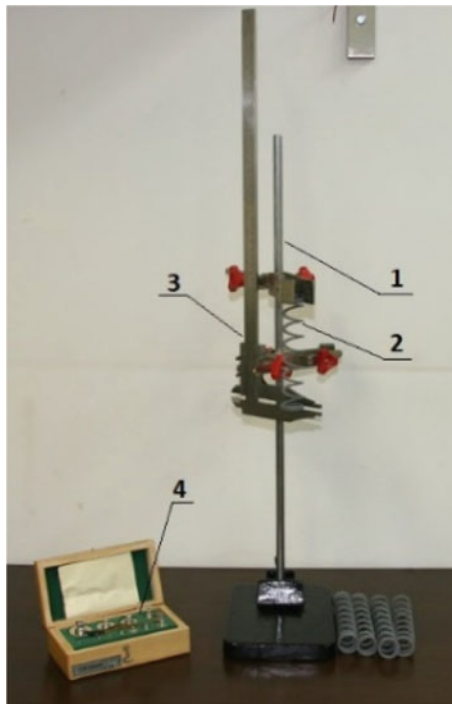


Fig. 6 Station for determining spring stiffness. 1—Stand, 2—test spring, 3—caliper, 4—weights



Fig. 7 Fixing and adjusting the spring to the correct height and stretching the spring with a 100 g weight

The determination of the stiffness coefficient was carried out in two stages, as shown in Fig. 7. In the first stage, the spring was fixed in the frame so that the lower ring of the spring was flush with the fixed part of the caliper with an accuracy of 0.05 mm. This made it possible to observe whether the spring would return to its original dimension after the load was removed.

In the next step, a 100 g weight was hung on the spring, and then the stretch value was read on the caliper. Due to the fact that the spring will not be stretched or compressed on the test stand, the value determined for such a minimum possible load of the stiffness coefficient k was considered the most appropriate. Performed experiments allows to calculate the stiffness coefficient for tested springs. The k value for E-4 and E-5 springs are 42 and 151 N/m respectively, for the rectangular profiles R-4 and R-5 are 62 and 227 N/m respectively and for circular profiles C-4 and C-5 are 231 and 454 N/m respectively. The results obtained will later help calculate the natural frequency of the springs for which the highest damping of pressure pulsations is obtained.

3 Tests on a Compressor Station

The tests were carried out on a test stand equipped with a Kaeser iComp9.Tower piston compressor. The compressor acts as a pulsating flow trigger. Figure 8 shows a diagram of the test pipeline with the spring mounting element and the place of mounting the sensors.

Pressure pulsation tests were performed using PCB Piezotronics sensors to measure dynamic pressures. All tests were performed for a discharge pressure of 5 bar and a rotational speed of the compressor drive shaft of 1100 rpm. Due to the specific work of the two pistons in the cylinders (on one crank of the crankshaft), the main excitation frequency resulted directly from the rotational speed of the shaft, so

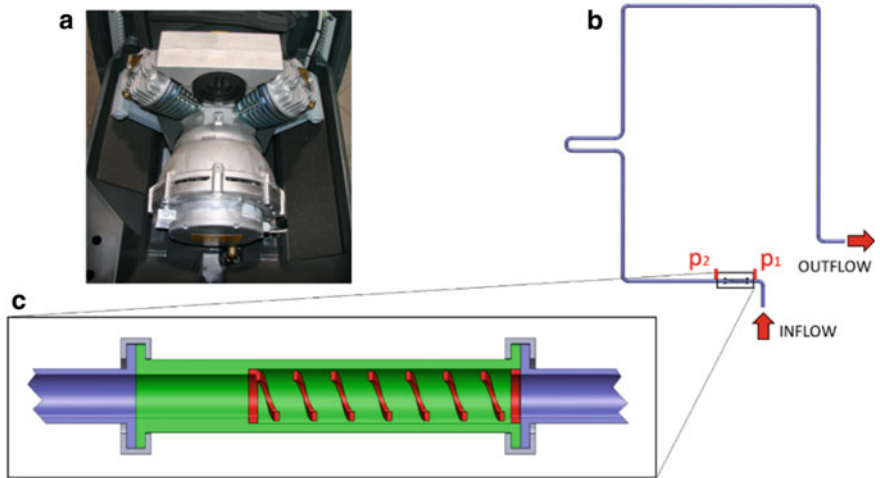


Fig. 8 Test stand. **a** Twin-cylinder reciprocating compressor. **b** Scheme of the test installation with the marked place of mounting of the flexible element and the sensors to measure dynamic pressures. **c** Method of installing the printed spring in the installation

it was about 18.3 Hz. Of course, due to the partial regulation of the compressor operation depending on the compressed gas discharge from the installation, this value during the tests could fluctuate within ± 0.5 Hz.

3.1 Test Results

The test results for the tested elements and the empty installation are presented in Table 1. These results show the values of pressure pulsation before and after the assembly place of the printed springs.

As can be seen in the table, a clear decrease in the amplitude of pressure pulsations was read for a spring with a round profile with a diameter of 5 mm. Other shapes also suppressed the pulsation value to a greater or lesser extent. The obtained results suggested possible significant attenuation of one of the main harmonic frequencies by the C-5 nozzle. Figure 9 presents the percentage values of the pressure pulsation damping for the total measured peak-to-peak value of the pulsation and for the amplitudes of the four main harmonics obtained from the Fourier analysis of the

Table 1 Peak-to-peak pressure pulsation values in front and behind the spring mounting point

Spring no	Empty (kPa)	E-5 (kPa)	R-5 (kPa)	C-5 (kPa)	E-4 (kPa)	R-4 (kPa)	C-4 (kPa)
Δp_1	45.98	44.34	44.36	40.41	43.21	43.11	42.99
Δp_2	45.71	44.85	44.18	40.69	44.00	44.10	43.76

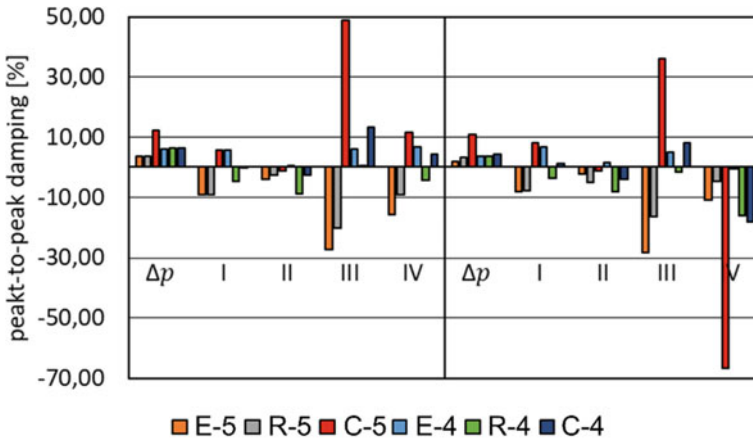


Fig. 9 Peak-to-peak damping for measured signal and the first four main harmonic values. Values for sensor in front of spring (left) and behind spring (right)

measured signal against the installation with a tubular element in place of the spring (Empty). The next harmonics correspond to the following values: 18.35 Hz; 36.7 Hz; 55 Hz; 73.35 Hz.

As can be seen, the C-5 spring attenuates the third harmonic of the signal the most, which for the measurement conditions is about 55 Hz. Due to the fact that the damping may result from the fundamental natural frequency in the axial direction of the spring, this value will be determined for the C-5 spring in the next chapter.

3.2 Determining the Fundamental Natural Frequency of a 3D Printed Spring

In order to determine the natural frequency of a coiled spring in the axial direction, it is necessary to know quantities such as: wire diameter (d), number of spring coils of the spring (N), diameter on which the wire is wound (D), density of the spring material (ρ) and its modulus of rigidity (G). Then, using the formula (1), the eigenfrequency can be determined [2]:

$$f_n = \frac{d}{4 \cdot N \cdot D^2} \cdot \sqrt{\frac{G}{2 \cdot \rho}} \tag{1}$$

In the case of a spring produced with 3D printing techniques, it is not easy to assess the modulus of rigidity value. For SLA printing techniques, this value should be constant throughout the print and in all directions, but it will depend not only on the resin used but also on the post-print processing process. For this reason, for

Table 2 Geometrical and material parameters of the spring C-5

Parameter	Value	Units
Wire diameter (d)	0.005	m
Mean diameter (D)	0.0207	m
Number of coils (N)	6.75	–
Material density (ρ)	1100	kg/m ³
Modulus of rigidity (G)	393.76	MPa

the presented considerations, this modulus was determined for the printed spring in accordance with Eq. (2) for calculating the stiffness coefficient (k) of compression/extension springs [8]:

$$k = \frac{G \cdot d^4}{8 \cdot N \cdot D^3} \quad (2)$$

Using the value of the spring stiffness coefficient C-5 determined as described in Sect. 2.2 and the geometric and material parameters of the spring, presented in Table 2, the modulus of rigidity G was determined for the printed spring and is also presented in Table 2.

Knowing the material and geometrical parameters of the spring, using the formula (1) after transformations, it was calculated that the natural frequency of the C-5 spring is 51.35 Hz.

The value calculated this way is largely based on the material values ρ and G of the printout determined by simple measurements. Both of these quantities cannot be determined in a very precise way due to the nature of the printed material. However, it can be seen that the value calculated for the C-5 spring is close to the value of the harmonic frequency best damped by this spring. For comparison, this value for the next circular spring was calculated as 45.25 Hz. This is a value between the 2nd and 3rd harmonics, but as shown in Fig. 9, in reality this value must be closer to the 3rd harmonic because for this frequency it shows pulsation attenuation. For springs with a rectangular wire cross-section, DIN 2090 should be used to read the shape factor ϵ . Due to the lack of significant attenuation of individual harmonics, calculations of f_n values for these springs will not be presented here.

4 Conclusions

The paper presents the possibility of using 3D printing techniques for the production of flexible elements such as springs. In particular, attention was paid to the complexity of this type of solution and the possibilities of producing springs with various “wire” profiles were presented. A significant disadvantage in this type of solution is, of course, the need to perform time-consuming processing of these types of printouts. Such printouts mounted inside the pipeline can be a significant novelty in terms

of suppressing pressure pulsations in compressor discharge pipelines. The springs do not generate a significant constriction in the installation which is an advantage compared to standard nozzles. In the scientific literature can be find information on the effectiveness of damping pressure pulsations with a frequency corresponding to the natural frequency of the flexible element. In the course of the research, it was noticed that indeed the C-5 spring with the natural frequency value of approx. 51.35 Hz dampens the nearest harmonic frequency of pulsation. Unfortunately, the method for determining this quantity is burdened with a certain error, which has not been estimated in this paper. The error is mainly due to uncertainty about the specific material characteristics of the post-processed print. Further work will focus on more accurate methods to determine the natural frequency of the printout and on checking printouts made of different resins.

Acknowledgements This research was funded by Polish National Centre for Research and Development, grant number LIDER/40/0140/L-11/19/NCBR/2020.

References

1. P. Młynarczyk, D. Brewczyński, J. Krajewska-Śpiewak, P. Lempa, J. Błądek, K. Chmielarczyk, Pressure pulsation and pipeline vibration damping with the use of 3D printed nozzles, *Mechanisms and Machine Science*, vol. 125 (Springer, 2022)
2. H.E. Oh, D.J. Park, W.B. Jeong, Numerical and experimental study on the reduction of refrigerant pressure pulsation within compressor pipes. *J. Sound Vib.* **438** (2019)
3. A. Zolfagharian, M. Lakhii, S. Ranjbar, Y. Tadesse, M. Bodaghi, 3D printing non-assembly compliant joints for soft robotics. *Results Eng.* **15**, 100558 (2022)
4. S. Herkal, M. Rahman, S. Nagarajaiah, V. Vedhan, J. Harikrishnan, P. Ajayan, 3D printed meta-materials for damping enhancement and vibration isolation: Schwarzites. *Mech. Syst. Signal Process.* **185**, 109819 (2023)
5. L. He, H. Peng, M. Lin, R. Konjeti, F. Guimbretière, J. Froehlich, Designing and controlling 3D printable springs, in *Ondulé: UIST '19*, 20–23 Oct (2019)
6. Ch. Jiao, G. Yan, Design and elastic mechanical response of a novel 3D-printed hexa-chiral helical structure with negative Poisson's ratio. *Mater. Des.* **212**, 110219 (2021)
7. A.S. Dalaq, M.F. Daqaq, Experimentally-validated computational modeling and characterization of the quasi-static behavior of functional 3D-printed origami-inspired springs. *Mater. Des.* **216**, 110541 (2022)
8. R.G. Budynas, K. Nisbett, *Shingley's Mechanical Engineering Design*, 9th edn. (The McGraw-Hill Companies, New York, 2012)